



UAV Mapping for Flood Routing in Steep and Densely Vegetated Areas: Insights from the Contok River Basin, Garang Watershed, Indonesia

Fahrudin Hanafi^{1*}, Edi Kurniawan¹, Dwi Priakusuma¹, Katarzyna Kubiak-Wojcicka²

¹Department of Geography, Faculty of Social and Political Sciences, Universitas Negeri Semarang, Indonesia

²Department of Hydrology and Water Management, Faculty of Earth Sciences and Spatial Management, Nicolaus Copernicus University in Torun (UMK), Poland

*Corresponding author's e-mail: fahrudin.hanafi@mail.unnes.ac.id

Received: 28 May 2024; Accepted: 26 June 2024; Published: 30 June 2024

Abstract: This research utilizes photogrammetry to assess flood routing dynamics in the Contok river basin, a sub-watershed with a challenging landscape characterized by steep slopes, dense vegetation, and meandering patterns. The objectives are to assess Unmanned Aerial Vehicle (UAV) mapping accuracy, evaluate the river's capacity for design flood volumes, quantify the impact of land cover changes on surface runoff, and provide insights for early warning systems and watershed conservation strategies. The study area, encompassing the Contok River Basin, a sub-watershed of the Garang Watershed, covers 7,413 km² and includes a stream length of 5,274 meters in Semarang City, Central Java, Indonesia. This research employed image processing of aerial photographs and satellite imagery. Aerial photos captured using UAV data were utilized to derive elevation data and cross-sectional profiles of the Contok River, essential for understanding channel morphology and hydraulic characteristics. Concurrently, satellite imagery was used for land cover analysis, identifying vegetation and built-up areas that influence surface runoff dynamics. Hydrological analysis was performed to quantify discharge magnitudes, simulated against river cross-sections to evaluate flood behavior under varying scenarios. Our proposed UAV mapping provides adequate accuracy for small and local areas. Furthermore, it remains reliable for flood routing analysis. We discovered that the capacity of the Contok River channel in the downstream area allows it to convey design flood discharges up to a 50-year return period, contrary to the upstream area, it overflows. Notably, the shift from vegetated to built-up and agricultural areas significantly contributes to the 10.6% increase in surface runoff. This research highlights the role of UAV-based photogrammetry in assessing and mitigating flood hazards amidst evolving land cover patterns. It also enhances the understanding of flood dynamics and thus provides insights that will serve as a reference for flood early warning systems, flood management practices, and watershed conservation.

Keywords: UAV-Mapping, Photogrammetry, Flood-Routing, Surface-Runoff, Land-Cover-Changes

DOI: <https://doi.org/10.55981/limnotek.2024.5028>

1. Introduction

Water resources management is the effort to plan, implement, monitor, and evaluate the administration of water resource conservation, utilization, and control of water damage (Indonesia, 2019). According to Triatmodjo (2008), water resources management is divided into two main activities: utilization and

regulation of water. Utilization of water resources focuses on using water for fulfilling needs such as clean water supply, irrigation, hydropower generation, water transportation, and so on. On the other hand, water regulation is oriented towards controlling water damage, ensuring that excess water does not lead to disasters (Triatmodjo, 2008).

The common phenomenon extensively studied regarding excess water is flooding. Flooding is a condition where the flow of a river exceeds the capacity of its channel, resulting in overflow or inundation (BSN, 2022). Suripin (2004) defines flooding as a condition where water exceeds the drainage channel's capacity or the flow of water in drainage channels is obstructed. Excess water can be caused by various factors, one of which is an increase in rainfall intensity, characterized by a dynamic and significant rise in precipitation (Kodoatie & Sugiyanto, 2002).

Floods are one of the disasters that occur quite frequently in Indonesia. Floods ranked third with a frequency of occurrence of 320 times, with the highest occurrence being 1,625 for forest and land fires followed by landslides with 360 occurrences (BNPB, 2023). Knowledge of potential flood threats is essential to provide early warnings, which can help in estimating community preparedness (BSN, 2022).

To estimate the potential flood threat, flood routing is commonly conducted. Flood routing is a method used to determine the timing and flow rate (hydrograph) at a specific point in the flow based on the upstream hydrograph (Triatmodjo, 2008). The determination of flow discharge is often approached using volume conservation, as seen in the Muskingum method for flood routing (Fenton, 2019). A simple method in flood routing uses a volume conservation approach, where the flow is considered as a prism. This method requires data on the flow discharge and the cross-sectional area of the stream (Fenton, 2019).

Accurate river cross-section data is necessary for flood routing. However, conducting geodetic terrestrial surveys for cross-section mapping is time-consuming, labor-intensive, and costly (Uysal *et al.*, 2015). Consequently, there is a lack of data on challenging landscapes characterized by steep slopes, dense vegetation, and meandering river patterns. Our Study area, the Contok Watershed, is situated on the lower slopes of Mount Ungaran, at an elevation ranging from 191 to 367 meters above sea level, with an average slope of 15% and a maximum slope of 35%. The river's total length across all orders is 9.246 kilometers, exhibiting a dendritic drainage pattern. Based on remote sensing

image analysis, nearly 60% of the Contok Watershed is covered with dense vegetation. Furthermore, 80% of the river channel is beneath the canopy cover, making direct aerial observations of the river channel are challenging.

The photogrammetry approach offers a solution for mapping in a remote, challenging landscape, and poorly mapped area. Photogrammetry combines art, science, and technology to obtain reliable information from photographic images (Lillesand & Kiefer, 1998; Rachmanto & Ihsan, 2020). Additionally, the use of photogrammetry with UAVs/drones is particularly suitable for large-scale measurement and mapping (Harfan *et al.*, 2019). In river morphometric data acquisition, photogrammetry processes overlapping aerial photos to create orthophoto maps and line maps (Marjuki *et al.*, 2019).

An orthomosaic procedure, as part of photogrammetry, corrects aerial photos geometrically to display objects accurately (Ikhwan *et al.*, 2021). Its primary purpose is to provide up-to-date visual information, identify specific objects, and monitor infrastructure conditions (Park *et al.*, 2022). Furthermore, orthomosaic techniques are valuable for large-scale mapping, including infrastructure, urban areas, disaster management, water resources, coastal regions, and forestry.

UAV-based photogrammetry efficiently captures detailed images of land cover, especially in small areas with low flight heights (Turner *et al.*, 2015). It can meet the demand for acquiring elevation data and orthophotomosaic with a high spatial resolution of up to 10 cm (Rusnák, *et al.*, 2018). Consequently, it has become an ideal method for assessing vegetation dynamics along riverbanks, analyzing river channel morphology after flooding, studying lateral river expansion, and reconstructing submerged channel topography (Dunford *et al.*, 2009; Hervouet *et al.*, 2011; Michez *et al.*, 2016; Tamminga *et al.*, 2015; Vericat *et al.*, 2009; Woodget *et al.*, 2014).

Mapping using UAV has significant importance in various scopes, such as cartography, environmental monitoring, and urban planning (Daud, *et al.*, 2022). The application of UAVs is also effective in erosion and flood surveys, as UAVs can continuously

produce 2D and 3D images in a short amount of time in the field (Duo *et al.*, 2018). Additionally, UAV can be used for continuous monitoring and mapping of natural disasters (Kim *et al.*, 2019).

Advanced technology, UAVs can assist in mapping by monitoring the elevation of the study area over time (Young *et al.*, 2021). In addition, UAVs are also considered more cost-effective with reasonably good accuracy compared to traditional surveys for spatial data collection (Hill, 2019).

The use of UAVs as data acquisition tools has been highly successful in the field of hydrology, particularly for modeling flood hydraulic characteristics. This success is bolstered by the high-resolution topographic data acquired from UAV mapping of river channels and floodplains (Feng *et al.*, 2015; Annis, *et al.*, 2020; Karamuz *et al.*, 2020). DEMs of topographic data are one of the primary sources used in hydraulic modeling and flood inundation mapping (Saksena & Merwade, 2015). DEM represents the elevation of the ground surface in the form of a digital model, which can be utilized to identify the slope or gradient of an area (Mabrur & Agustina, 2022). This data is essential for representing information about land surfaces that have been inundated or showing the direction of water flow during floods. Therefore, data acquisition using UAV platforms can enhance the effectiveness of preventive and systematic disaster management (Kim *et al.*, 2019).

Nevertheless, research on flood routing in steep, densely vegetated areas is limited. While many studies have examined flood dynamics across various terrains, the unique characteristics of regions with extreme slopes and dense vegetation are understudied. Previous research has focused on flat or moderately sloped areas, neglecting specific aspects such as the effects of steep slopes on infiltration, evapotranspiration, and flow resistance by vegetation. This study addresses this gap by using aerial photography for detailed hydrological and topographical analysis. There is an urgent need for more research to develop accurate aerial photo-based models and effective flood mitigation strategies for steep, vegetated regions.

Therefore, the research objectives are to: first, assess the accuracy of UAV mapping in a challenging setting, such as a steep and densely vegetated river basin; second, conduct a flood routing analysis to evaluate the storage capacity of the Contok River channel for the design flood volume; and third, quantify the impact of land cover changes on surface runoff. This research is expected to provide insights that will serve as a reference for early warning systems against flood threats and for watershed conservation.

2. Materials and Methods

This research employed two analyses: photogrammetric analysis, hydrological analysis. Photogrammetric analyses were used to determine the river's cross-sectional profile, while hydrological analysis will be conducted to obtain flood routing results. In addition, a remote sensing data series was used to identify the change in the runoff coefficient.

2.1 Study Area

The research location is Contok Watershed, which is a sub-watershed of the Garang Watershed. The Contok Watershed has an area of 7,413 km² with 5,274 km of stream length, located in Patemon and Sekaran Village, Gunungpati District, Semarang City, Central Java Indonesia. Figure 1 is the map of the study area.

2.2. Photogrammetric Analysis

In this study, photogrammetric mapping aims to establish a geometric relationship between an object and an aerial photograph/image and derive spatial information about the object under study from the photograph. The photogrammetry process yields data in the form of land features captured through aerial photography. Photogrammetry processes data quickly and with high quality (Sutjipto *et al.*, 2017). According to Putra *et al.* (2023) The photogrammetric mapping resulting data includes various models such as the Digital Elevation Model (DEM), Digital Terrain Model (DTM), and Digital Surface Model (DSM).

The processing of aerial photos from UAVs was conducted using Agisoft Metashape software (<https://www.agisoft.com/>). This software was used for image processing of UAV acquisition data through the formation of

mosaics with automatic tie point input, the formation of three dimensions (point cloud), and the extraction of DEM from the orthophoto. The output produced is a three-dimensional representation of the surface with coordinates X, Y, and Z. The resulting orthomosaic is then tested using the root mean square error

(RMSE) method, which involves comparing the total difference in point displacements to the number of sampled points. The accuracy values are classified according to the Regulation of the Indonesian Geospatial Information Agency (BIG) number 15 of 2014 (BIG, 2014) as shown in Table 1.

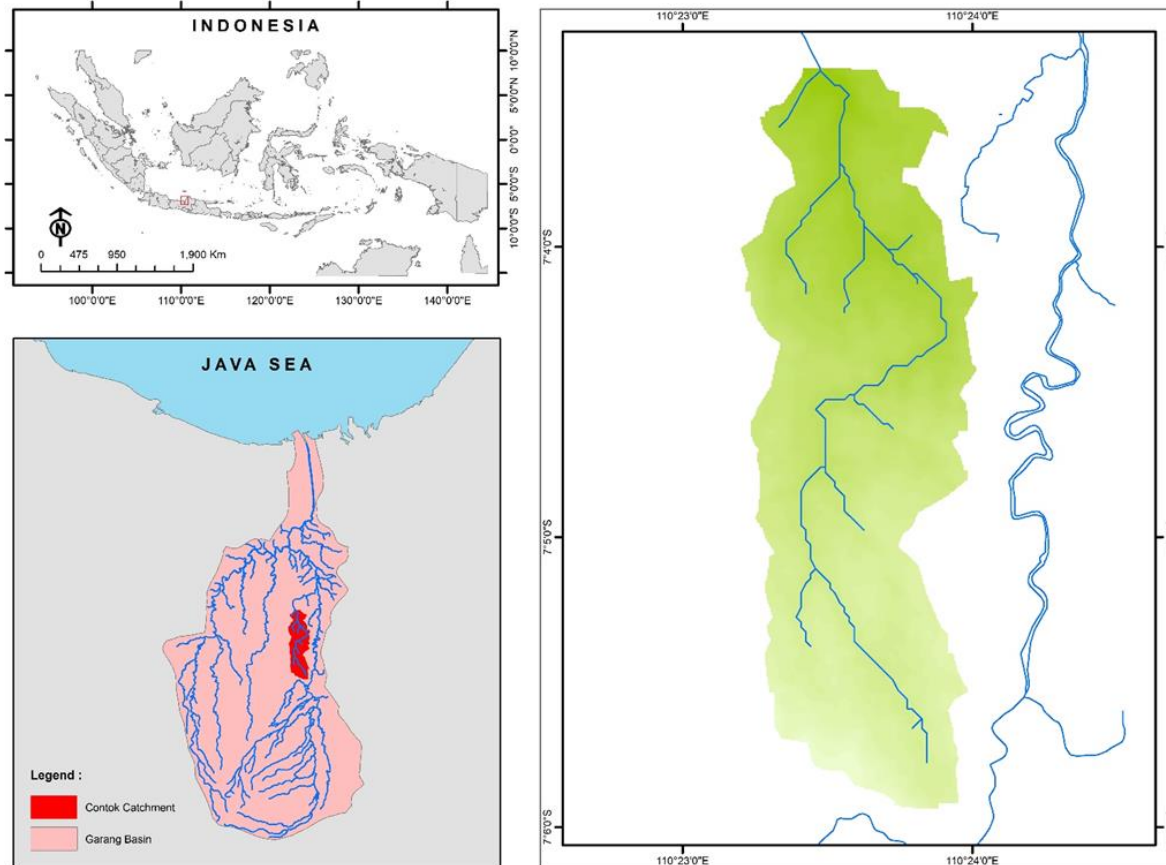


Figure 1. Map of the Study area, Contok River Basin, a Sub-Watershed of Garang Watershed, Indonesia

Table 1. Classification of Map Accuracy

No.	Scale	Accuracy Map of RBI		
		Class 1 CE90 (m)	Class 2 CE90 (m)	Class 3 CE90 (m)
1	1: 1,000,000	200	300	500
2	1: 500,000	100	150	250
3	1: 250,000	50	75	125
4	1: 100,000	20	30	50
5	1: 50,000	10	15	25
6	1: 25,000	5	7,5	12,5
7	1: 10,000	2	3	5
8	1: 5,000	1	1.5	2.5
9	1: 2,000	0.5	0.75	1.25
10	1: 1,000	0.2	0.3	0.5

Source: (BIG, 2014)

2.3 Flood Routing

Flood routing was conducted using rainfall data from Climate Hazards Group InfraRed Precipitation with Station data (CHIRPS) covering 20 years, from 2003 to 2022, retrieved from the Climate Hazard Centre, UC Santa Barbara website (UCSB, 2023). The design flood was analyzed for 25-year and 50-year return periods, using the rational method calculation.

To track the river's storage volume in response to accommodate the design flood discharge, the Manning method was employed. By examining the flow velocity values based on the river bed slope and cross-sectional area, simulations were conducted to assess the river's storage capacity against 25 and 50-year design flood discharges.

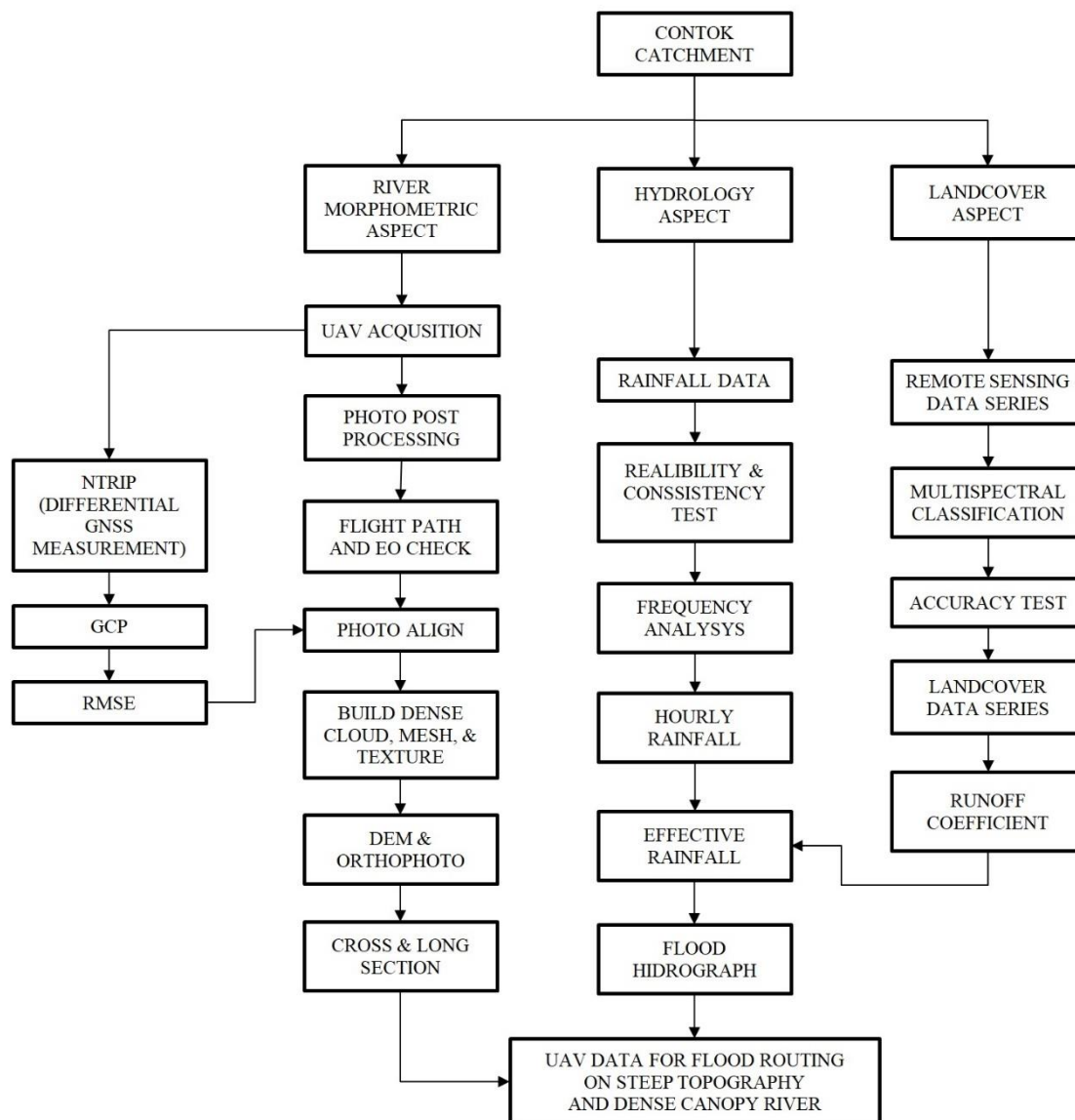


Figure 2. Flowchart diagram of the flood routing study using UAV data, precipitation data, and remote sensing data series in the steep and densely vegetated areas of the Contok river basin, a sub-watershed of the Garang Watershed, Semarang, Central Java, Indonesia

There are several methods used in design flood calculation, i.e. Mononobe method for effective rainfall calculation (Equation 1), Kirpich method for time of concentration calculation (Equation 2), Rational method for design flood calculation (Equation 3), Manning method for defining the stream velocity based on the steepness of the river cross-sectional profile and its natural condition (Equation 4). Generally, the more cross-sectional profiles will result in a more precise simulation.

$$I = \left[\frac{R_{24}}{24} \right] \times \left[\frac{24}{t_c} \right]^{2/3} \quad \dots \text{Eq. 1}$$

where, I : effective rainfall (mm), R_{24} : design rainfall (mm), t_c : time of concentration (hour).

$$t_c = 0,01947 \times L^{0,77} \times S^{-0,385} \quad \dots \text{Eq. 2}$$

where, t_c : time of concentration (hour), L : river/stream length (m), and S : riverbed steepness/slope.

$$Q = 0,278 \times C \times I \times A \quad \dots \text{Eq. 3}$$

where, Q : design flood (m³/s), C : runoff coefficient, I : effective rainfall (mm), A : catchment area (km²).

$$v = \frac{1}{n} \times R^{2/3} \times S^{1/2} \quad \dots \text{Eq. 4}$$

where, v : stream velocity (m/s), n : Manning roughness coefficient, R : Hydraulic radius, S : slope.

Figure 2 shows a summary of each step used in this research. Image processing is conducted for both aerial photographs and satellite imagery. Aerial photographs were processed to obtain the elevation data and the cross-sectional profiles of the Contok river, while satellite imageries were used for land cover identification analysis. On the other hand, hydrological analysis was performed to determine the discharge magnitude and further simulated against the river cross-section profiles. This study serves as a flood mitigation effort, by identifying areas of the river with

lower capacity due to variations in cross-sectional heights (velocity) in comparison to the flood magnitude.

3. Result and Discussion

3.1. River Morphometric aspect

The aerial images collected in this research total approximately 720 photos, captured over two flights to cover the entire study area as shown in Figure 3. Each flight was conducted with specifications of GSD: 2,73 cm/pixel, Flight altitude: 100 m, Flight area 965x346 m, Photo overlap: 70%, and Flight time: 15 minutes 30 seconds.



Figure 3. UAV flights path to cover the Contok River Basin, a sub-watershed of Garang River, Central Java Indonesia

Modeling and Ortho mosaicking processes from aerial photos resulted in a block photo of the research area with a DEM built based on UAV's inherent coordinate values. The orthomosaic data is in raster form, providing information in pixel-based form. To obtain more specific quantitative data, transforming raster data into vector data is necessary. This process converts the Orthomosaic raster data into vector data to identify the length and area of the studied objects. Figure 4 shows the results of the Ortho-mosaicking process.

Figure 5 provides spatial and elevation data resolution of 0.05m. The subsequent analysis conducted is planimetric testing to determine the data quality level from the post-processing of aerial photos. Planimetric testing is carried out by testing the positional accuracy referring to the actual coordinates at the test points on the ground surface. The control points used are Independent Control Points (ICP). The planimetric testing results are presented in Table 2.

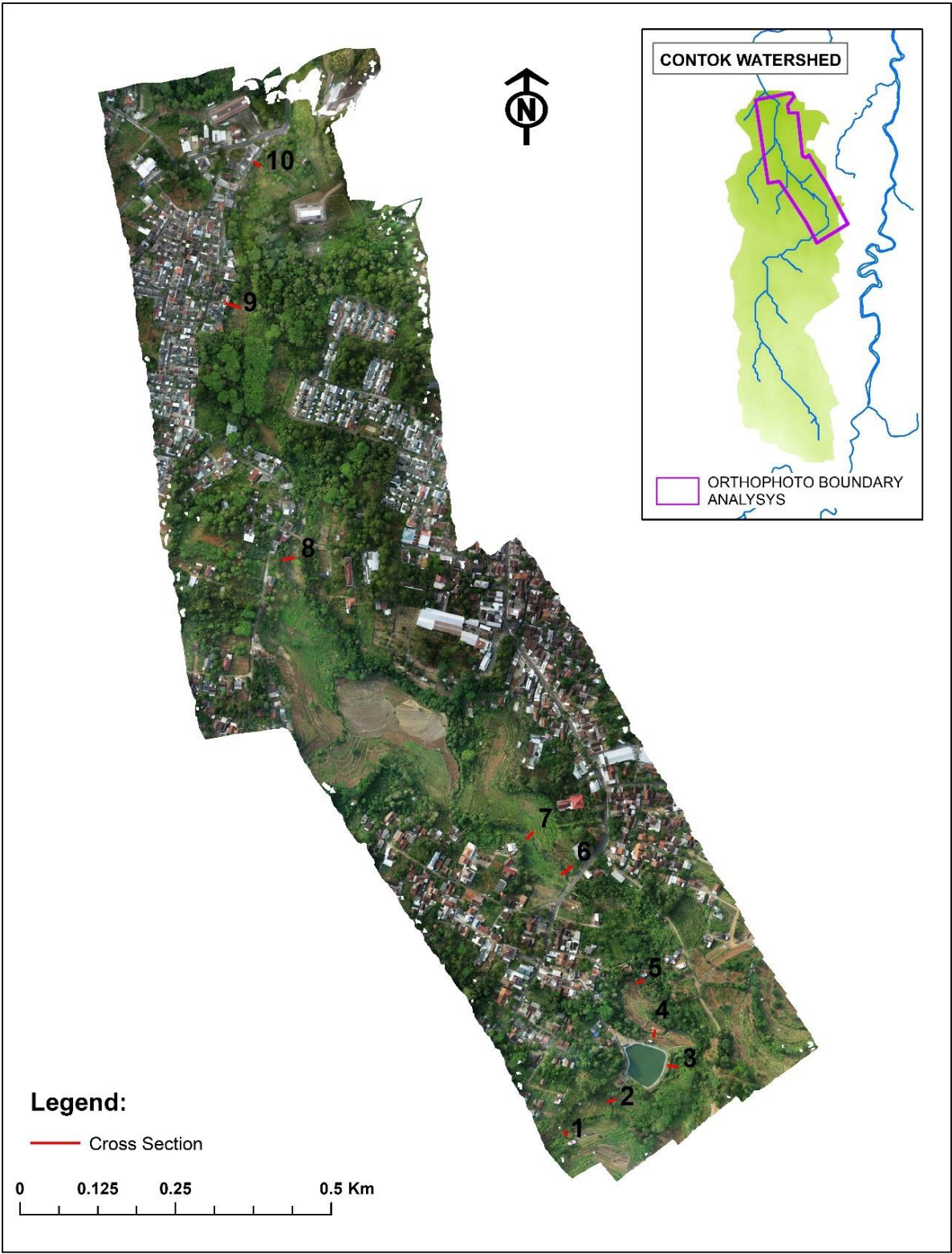


Figure 4. Orthomosaic and cross-sectional location (marked in Red) of Contok River Basin, a sub-watershed of Garang River, Central Java Indonesia

Table 2. Planimetric test

No	Image Distance (m)	Real Distance (m)	Difference (m)
1	4.249	4.395	0.146
2	3.757	3.840	0.083
3	4.341	4.435	0.094
4	3.604	3.640	0.036
5	4.330	4.435	0.105
6	4.000	4.045	0.045
7	4.859	4.890	0.031
8	4.215	4.395	0.180
Displacement Distant Total		0.720	
Planimetric Test Result		0.300	

The DEM extracted from the orthophoto post-processing after the 3D point cloud was generated, was then used to create cross-sectional data of the river within the most opened area. Figure 5 is the DEM map with the locations of the river cross-sections. Figure 6 is an example of the generated cross-sectional profile.

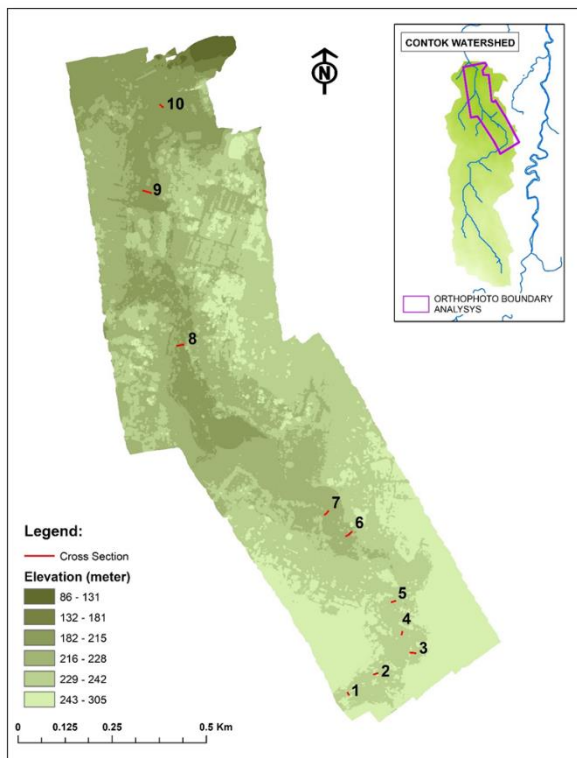


Figure 5. The Digital Elevation Model (DEM) map along with the locations of the river cross-sections.

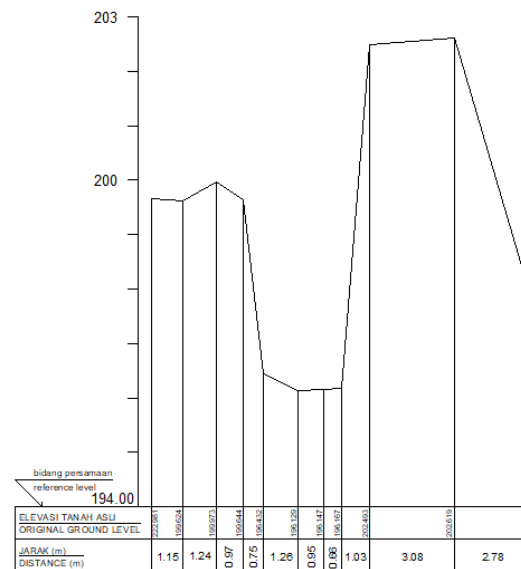


Figure 6. Cross Section on Control Point

The map produced from this research falls under the category of large-scale maps, namely 1:10,000. Referring to the standards of the BIG as shown in Table 1, the map resulting from orthomosaic processing in this study falls under Class 1 accuracy. The planimetric test applied through the ICP control method yields a displacement value of 0.3 m (Table 2), which is below the threshold of the BIG accuracy criteria, which is 2 m. ICP measurement was conducted by performing a manual survey using measuring tape on the easily recognized objects both in aerial photos and in the field. For example, the bridge width serves as a control point for the river section, as do the street corners at certain locations. Overall, eight places were measured as ICP.

The application of UAV mapping in this study involved Ground Control Points (GCPs) to align and scale the photogrammetric data correctly by providing reference points that the software uses to correct any distortions and ensure spatial accuracy. Good accuracy also can be achieved through favorable weather conditions, optimal flying altitude, and well-suited non-vegetative areas for control purposes. In this study, a total of 12 Ground Control Points (GCPs) were measured using the GNSS (Global Navigation Satellite System) NTRIP (Networked Transport of RTCM via Internet Protocol) method, with a Sokkia GRX-2 as the rover and the Telkom Simpang Lima CORS as the base station.

This study demonstrates that the use of ICP in photogrammetry remains effective for narrow river catchments. The advantage of the ICP method in narrow areas lies in the ease of field verification of objects that are easily recognizable both from aerial photos and on the ground. The use of GCP in this study was less effective due to the reliance on the NTRIP (stop and go) method, which depends on internet connectivity. In areas with moderate to steep slopes and dense vegetation cover, this dependence leads to signal distortion, resulting in poor location accuracy with intolerable RMSE (Root Mean Square Error). On the other hand, some of the GCPs are unseen from the aerial photos due to the densely vegetated area. Consequently, this study indicates that ICP is effective for photogrammetry in small areas, whereas GCP with static location measurement methods is required for larger areas.

3.2. Landcover and precipitation aspects

Land cover data in the Contok Watershed is required for the analysis of run-off coefficients in flood routing. Land cover is associated with the direction of river flow from upstream to downstream. Identification of land cover is conducted through the multispectral classification of Sentinel-2 imagery, using supervised classification maximum likelihood. This method falls under digital classification types because data processing is based on the digital values of images using specific software. The principle used is to group pixels with similar spectral characteristics into the same category or class for identification through a

distinguishing color (Gibson & Power, 2000; Marini *et al.*, 2014). The Landcover map of 2013 and 2023 are shown in Figure 7, while the tabular comparison is shown in Table 3.

Table 3. Comparison of Land Cover in the Contok Watershed in 2013 and 2023

No	Land Cover	2013 (km ²)	2023 (km ²)
1	Built Area	1.416	1.914
2	Open Area	0.086	0.173
3	Agriculture	0.421	0.923
4	Vegetation	0.590	4.402
Total		7.413	7.413

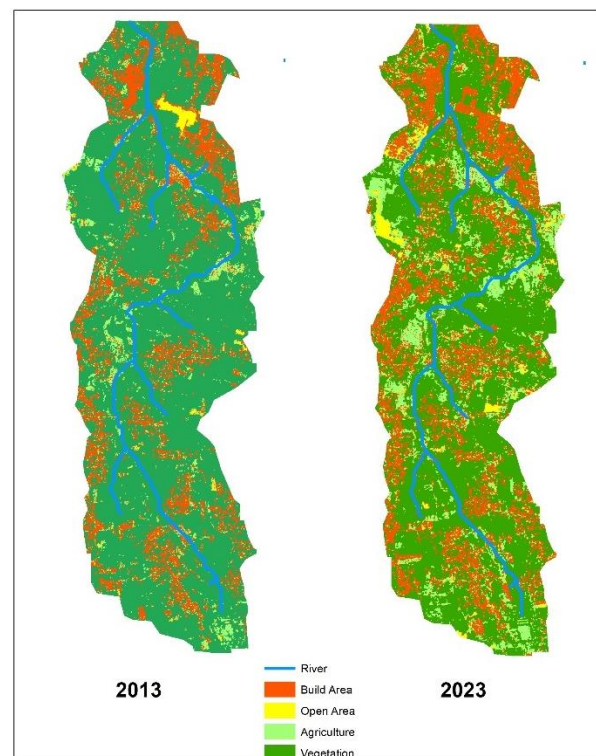


Figure 7. Comparison Land Cover in the Contok watershed in 2013 and 2023, resulted from the Sentinel-2 imagery multispectral classification

Frequency analysis was conducted on rainfall data from CHIRPS to obtain rainfall magnitudes with return periods of 25 and 50 years. Using watershed parameters of land cover (Table 3), the length of the river segment, riverbed slope, the coefficient of run-off analysis, concentration time, and effective rainfall are then analyzed and resulted in the runoff coefficient (C) of the Contok Watershed as shown in Table 4.

Table 4. The runoff coefficient (C) of the Contok Watershed

No	Land Cover	2013			2023		
		Area (km ²)	C	Composite	Area (km ²)	C	Composite
1	Built Area	1,416	0,5	0,098	1,914	0,5	0,129
2	Open area	0,086	0,3	0,004	0,173	0,3	0,007
3	Agriculture	0,421	0,3	0,017	0,923	0,3	0,037
4	Vegetation	5,490	0,2	0,148	4,402	0,2	0,119
Total		7,413		0,264	7,413		0,292

3.2. Hydrology aspect

The Contok Watershed area has a length of 5,274 meters, with a riverbed (based on long section analysis) slope of 0.0207. The concentration-time value is determined to be 63.68 minutes or 1.06 hours. Based on this concentration time value, effective rainfall is analyzed using the Mononobe method (Equation 1). The effective rainfall values for each return period are obtained as shown in Table 5.

Table 5. The results of effective rainfall analysis and discharge

Return Period (year)	Rain (mm)	Effective Rain (mm)	Q 2013 (m ³ /s)	Q 2023 (m ³ /s)
25	118,088	39,354	21,418	23,698
50	130,463	43,468	23,662	26,181

The calculated design flood discharge results for the years 2013 and 2023 with return

periods of 25 and 50 years are presented in Table 5. The Manning equation is used to simulate river storage based on cross-sectional profiles and flow velocities. The coefficient of roughness for the natural channel with vegetation obstruction is 0.07, and the cross-sectional area (Figure 5) is 12.06 m². Therefore, the channel storage capacity is 25.38 m³ s⁻¹.

The same storage capacity calculations were conducted for the other ten cross-section points, to determine the storage capacity representing the upstream, middle, and downstream of Contok Watershed.

Table 6 shows the river storage capacity analyzed at each cross-section based on the Manning equation (Equation 4). The storage capacity is then simulated against a discharge with a return period of 50 years in 2023. The simulation of storage volume at each cross-section is shown in Figure 8 to 17.

Table 6. Storage simulation for each cross-section

Location	Area (m ²)	P (m)	V (m/s)	Capacity (m ³ /s)	Q25-2023 (m ³ /s)
CS 1	5.25	6.52	1.78	9.33	26.18
CS 2	7.90	7.41	2.14	16.94	26.18
CS 3	15.69	12.77	2.36	36.95	26.18
CS 4	8.57	9.42	1.93	16.52	26.18
CS 5	5.10	9.03	1.40	7.15	26.18
CS 6	25.58	16.69	2.73	69.84	26.18
CS 7	11.24	10.03	2.22	24.89	26.18
CS 8	15.95	11.64	2.53	40.42	26.18
CS 9	13.65	10.65	2.42	33.09	26.18
CS 10	12.06	9.73	2.37	28.58	26.18

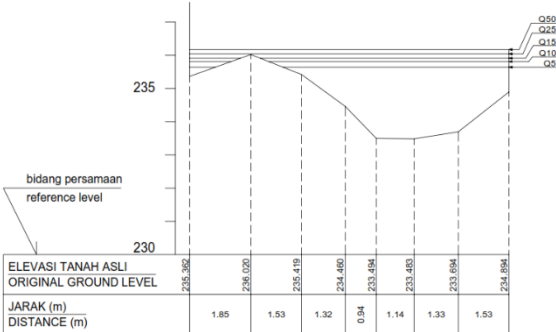


Figure 8. Storage simulation for cross-section 1

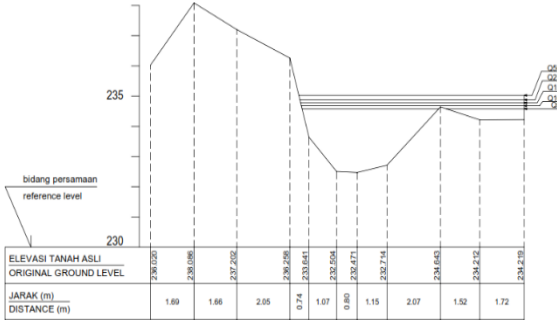


Figure 9. Storage simulation for cross-section 2

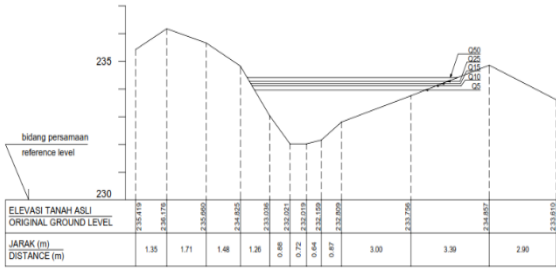


Figure 10. Storage simulation for cross-section 3

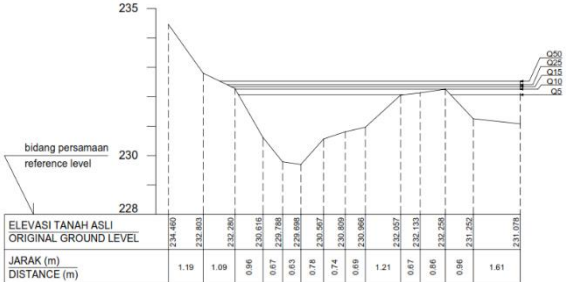


Figure 11. Storage simulation for cross-section 4

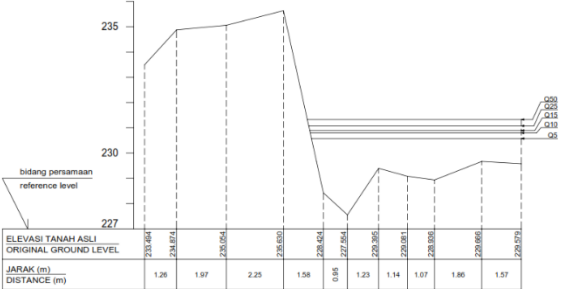


Figure 12. Storage simulation for cross-section 5

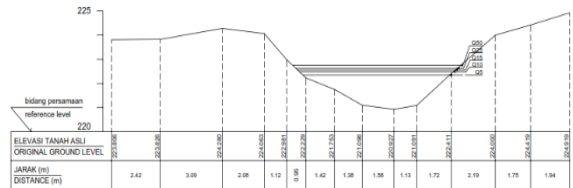


Figure 13. Storage simulation for cross-section 6

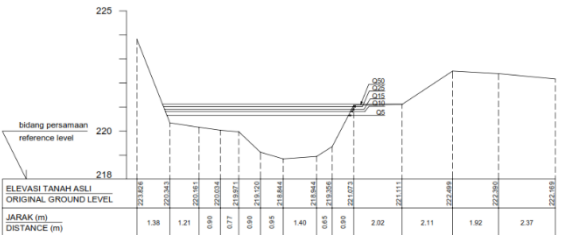


Figure 14. Storage simulation for cross-section 7

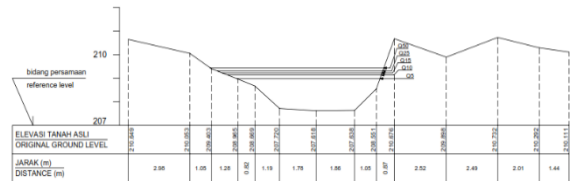


Figure 15. Storage simulation for cross-section 8

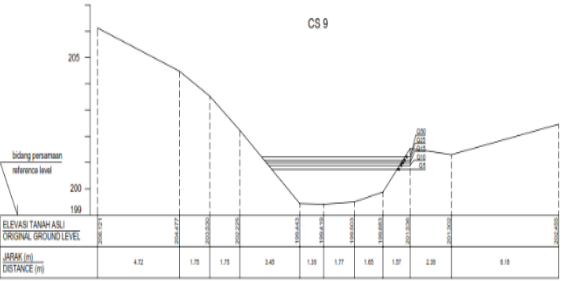


Figure 16. Storage simulation for cross-section 9

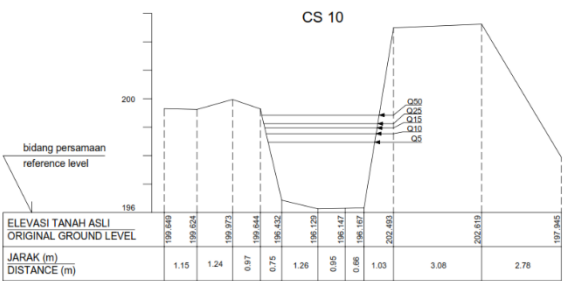


Figure 17. Storage simulation for cross-section 10

3.3. Landcover change aspect

Land cover changes are an important factor in increasing surface runoff. This is supported by several previous studies; deforestation and urbanization are the most influential factors in changing hydrological cycles and sedimentation (Siswanto & Frances, 2019). Changes in land cover, especially in built-up areas, greatly affect the magnitude of surface runoff (Sidiq, *et al.*, 2022).

Massive changes in land cover occur with a reduction in vegetation area of 1.01 km², converting it into built-up areas and agricultural land. These changes trigger changes in the runoff coefficient and increase the results of the design flood analysis by 10,6%. The downstream section of the Contok River in the study area is still capable of accommodating the 50-year return period flood discharge for the 2023 simulation, with overflow occurring only at cross-sections 1, 2, 4, and 5. This is due to field conditions, where the upstream area has small channels with banks that are either fallow land or have been utilized as fields, while in the downstream area, embankments have been constructed, along with river channel improvements.

4. Conclusion

The research findings indicate that UAV mapping without GCPs provides adequate accuracy for small and local areas. However, for larger areas with extensive flight paths, GCPs are necessary, especially for river mapping on steep slopes with dense vegetation, and meandering patterns. Special treatments are required to obtain sequential and continuous cross-sections with integrated elevation, during aerial photography and post-processing. Further research could focus on integrating multi-return LiDAR with photogrammetric point clouds to improve accuracy in dense vegetation areas. Developing automated algorithms for vegetation point filtering in photogrammetry, possibly using machine learning, would enhance efficiency. Comparative studies among LiDAR, filtered photogrammetry, and vegetation indices could validate their performance in varied environments. Exploring advanced remote sensing technologies like hyperspectral imaging or radar systems could

further advance canopy removal and land elevation mapping capabilities.

The capacity of the Contok River channel in the downstream area is still able to convey design flood discharges up to a 50-year return period, while in the upstream area, it overflows. A significant factor in increasing surface runoff in this study is the change in land cover. The change in land cover from vegetated areas to built-up and agricultural areas increases surface runoff by 10.6%. To minimize flooding at specific cross-sections and return periods, it is necessary to construct river embankments and optimize reservoirs, considering land use changes beyond our control.

Data availability statement

The topographic data of the river and aerial photographs utilized in this study were obtained through direct measurements. Rainfall data were sourced from the Central Java Public Works Department and the UCSB Climate Hazards Center - CHIRPS website (<https://www.chc.ucsb.edu/data/chirps>).

Funding Agencies

This research was supported by the Department of Geography and the Faculty of Social and Political Sciences, Universitas Negeri Semarang, Indonesia.

Conflict of interests

All authors declare that there are no conflicts of interest in this study.

Acknowledgment

Special thanks to the Kobra Sekempol Survey Team and CV. Sembilan Samudera for their contributions in terms of equipment, effort, and expertise.

References

- Annis A, Nardi F, Petroseli A, Apollonio C, Arcangeletti E, Tauro F, Grimaldi S. 2020. UAV DEMs for Small Scale Flood Hazard Mapping. *Water*. <https://doi.org/10.3390/w12082232>
- Badan Informasi Geospasial-BIG. 2014. Peraturan Kepala BIG Nomor 15 Tahun 2014 tentang Pedoman Teknis Ketelitian Peta Dasar. Jakarta: BIG. In Bahasa
- Badan Nasional Penganggulangan Bencana-BNPB. 2023. Data Informasi Bencana Indonesia.

- LIMNOTEK Perairan Darat Tropis di Indonesia 2024 (1), 5; <https://doi.org/10.55981/limnotek.2024.5028>
Retrieved December 18, 2023, from <https://dibi.bnpp.go.id/> In Bahasa
- Badan Standardisasi Nasional-BSN. 2022. SNI 8840-3:2022 Sistem Peringatan Dini Bencana - Bagian 3: Banjir. Jakarta: Badan Standardisasi Nasional. In Bahasa
- Daud SM, Yusof MY, Heo CC, Khoo LS, Singh MK, Mahmood MS, Nawawi H. 2022. Applications of Drone in Disaster Management: A Scoping Review. *Science Justice*, 62, 30-42. <https://doi.org/10.1016/j.scijus.2021.12.001>
- Dunford R, Michel K, Gagnage M, Piégay H, Trémelo ML. 2009. Potential and Constraints of Unmanned Aerial Vehicle Technology for The Characterization of Mediterranean Riparian Forest. *International Journal of Remote Sensing*, 4915-4935. <https://doi.org/10.1080/01431160903023025>
- Duo E, Trembanis AC, Dohner S, Grotoli E, Caviola P. 2018. Local-scale Post-event Assessments with GPS and UAV-based Quick-response Surveys: A Pilot Case From The Emilia-Romagna. Italy) Coast. *Natural Hazard and Earth System Sciences*, 18(11), 2969-2989. <https://doi.org/10.5194/nhess-18-2969-2018>
- Feng Q, Liu J, Gong J. 2015. Urban Flood Mapping Based on Unmanned Aerial Vehicle Remote Sensing and Random Forest Classifier—A Case of Yuyao, China. *Water*. <https://doi.org/10.3390/w7105377>
- Fenton JD. 2019. Flood Routing Methods. *Journal of Hydrology*, 570, 251-264. <https://doi.org/10.1016/j.jhydrol.2018.12.073>
- Gibson PJ, Power CH. 2000. Introductory Remote Sensing: Digital Image Processing and Applications. New York: Routledge.
- Harfan A, Yudhatama D, Bachrodin I. 2019. Pemanfaatan Metode Fotogrametri Untuk Pengukuran Garis Pantai dan Identifikasi Objek-objek Tematik dengan Menggunakan Wahana UAV. Unmanned Aerial Vehicle. Studi Kasus Pengukuran Garis Pantai di Pangkalan TNI AL Pondok Dayung. *Jurnal Chart Datum*, 71-84. In Bahasa
- Hervouet A, Dunford R, Piégay H, Belletti B, Trémelo ML. 2011. Analysis of Post-flood Recruitment Patterns in Braided-Channel Rivers at Multiple Scales Based on an Image Series Collected by Unmanned Aerial Vehicles, Ultra-light Aerial Vehicles, and Satellites. *GIScience Remote Sensing*, 50-73. <https://doi.org/10.2747/1548-1603.50.1.50>
- Hill AC. 2019. Economical Drone Mapping For Archeology: Comparison of Efficiency and Accuracy. *Journal of Archeological Science: Reports*, 24, 80-91. <https://doi.org/10.1016/j.jasrep.2018.11.021>
- Ikhwan M, Ratnaningsih A, Lestari I, Ikhsani H. 2021. Aplikasi Teknologi Unmanned Aerial Vehicle. UAV) untuk Mengidentifikasi Tutupan Hutan dan Lahan di Universitas Lancang Kuning. *Wahana Forestra Jurnal Kehutanan*, 86-101. <https://doi.org/10.20886/jphh.2020.38.1.41-53>
In Bahasa
- Indonesia. 2019. Undang-undang Nomor 17 Tahun 2019 tentang Sumber Daya Air. Jakarta: Kementerian Hukum dan HAM. In Bahasa
- Karamuz E, Romanowicz RJ, Doroszkiewicz J. 2020. The Use of Unmanned Aerial Vehicles in Flood Hazard Assessment. *Journal of Flood Risk Management*. <https://doi.org/10.1111/jfr3.12615>
- Kim SS, Kim TH, Sim JS. 2019. Applicability Assessment of UAV Mapping for Disaster Damage Investigation in Korea. *The International Archives of the Photogrammetry Remote Sensing and Spatial Information Science*, 209-214. <https://doi.org/10.5194/isprs-archives-XLII-3-W6-209-2019>
- Kodoatie RJ, Sugiyanto. 2002. Banjir: Beberapa Penyebab dan Metode Pengendaliannya dalam Perspektif Lingkungan. Yogyakarta: Pustaka Pelajar. In Bahasa
- Lillesand TM, Kiefer RW. 1998. Penginderaan Jauh dan Interpretasi Citra. 4 ed. Yogyakarta: Gadjah Mada University Press. In Bahasa
- Mabrur AY, Agustina F. 2022. Pemetaan Orthophoto untuk Rencana Pembuatan Peta Rawan Longsor. *Jurnal Ilmiah Universitas Batanghari Jambi*, 408-411. <https://doi.org/10.33087/jiubj.v21i2.1630> In Bahasa
- Marini Y, Emiyati, Hawariyah S. 2014. Perbandingan Metode Klasifikasi Supervised Maximum Likelihood dengan Klasifikasi Berbasis Objek untuk Inventarisasi Lahan Tambak di Kabupaten Maros. *Prosiding Seminar Nasional Penginderaan Jauh 2014*, 505-516. In Bahasa
- Marjuki B, Astutik S, Hartini KS, Wijanarko SR, Prananingtyas SR, Ridha MR, Ananda R. 2019. Pemetaan menggunakan UAV. Pusdatin Kementerian PUPR Indonesia.
- Michez A, Piégay H, Lisein J, Claessens H, Lejeune P. 2016. Classification of Riparian Forest Species and Health Condition Using Multi-temporal and Hyperspatial Imagery from Unmanned Aerial System. *Environmental Monitoring and Assessment*. <https://doi.org/10.1007/s10661-016-5282-0>
- Park J, Cho YK, Kim S. 2022. Deep learning-based UAV image segmentation and inpainting for generating vehicle-free orthomosaic. *International Journal of Applied Earth*

- LIMNOTEK Perairan Darat Tropis di Indonesia 2024 (1), 5; <https://doi.org/10.55981/limnotek.2024.5028>
Observation and Geoinformation.
<https://doi.org/10.1016/j.jaq.2021.102520>
- Putra RS, Riani D, Silitonga SP. 2023. Pembuatan Digital Elevation Model Universitas Palangka Raya Menggunakan Drone dan GPS Geodetik. *Jurnal Basement*, 1, 33-40. <https://doi.org/10.1016/j.basment.2023.01.004>
 In Bahasa
- Rachmanto DH Ihsan M. 2020. Pemanfaatan Metode Fotogrametri Untuk Pemetaan Skala 1: 1000. Studi Kasus: Universitas Pendidikan Indonesia. *Jurnal ENMAP*, 81-86. <https://doi.org/10.30630/enmap.v2i2.34>
- Rusnák M, Sládek J, Kidová A, Lehotský M. 2018. Template for high-resolution river landscape mapping using UAV technology. *Measurement*, 139-151. <https://doi.org/10.1016/j.measurement.2018.02.036>
- Saksena S, Merwade V. 2015. Incorporating the effect of DEM resolution and accuracy for improved flood inundation mapping. *Journal of Hydrology*, 180-194. <https://doi.org/10.1016/j.jhydrol.2015.08.021>
- Sidiq W, Hanafi F, Priakusuma D, Haruman W, Sumarso M, Setyowati N. 2022. Analisis Banjir Genangan di Kawasan Tembalang dan Sekitarnya. *Jurnal Riptek*, 137-144. <https://doi.org/10.31289/ripteck.v2i1.4261>
- Siswanto SY, Frances F. 2019. How land use/land cover changes can affect water, flooding and sedimentation in a tropical watershed: a case study using distributed modeling in the upper Citarum Watershed, Indonesia. *Environmental Earth Sciences*, 78(17), 1-15. <https://doi.org/10.1007/s12665-019-8575-7>
- Suripin. 2004. Sistem Drainase Perkotaan yang Berkelanjutan. Yogyakarta: Andi Offset. In Bahasa
- Sutjipto AT, Purwiyono TT, Azizi MA. 2017. Monitoring Pergerakan Massa Batuan Dengan Metode Terestris Menggunakan Total Station Dan Metode Fotogrametri Di Kaliwadas, Kebumen, Jawa Tengah. Workshop Seminar Nasional Geomekanika 4. Padang. In Bahasa
- Tamminga AD, Eaton BC, Hugenholtz CH. 2015. UAS-based remote sensing of fluvial change following an extreme flood event. *Earth Surface Processes and Landforms*, 1464-1476. <https://doi.org/10.1002/esp.3940>
- Triatmodjo B. 2008. Hidrologi Terapan. Cetakan Kedua ed.. Yogyakarta: Beta Offset.
- Turner D, Lucieer A, De-Jong SM. 2015. Time Series Analysis of Landslide Dynamics Using an Unmanned Aerial Vehicle. UAV. *Remote Sensing*, 1736-1757. <https://doi.org/10.3390/rs70301736>
- UCSB Climate Hazards Center. 2023. Climate Hazards Group InfraRed Precipitation with Station data. CHIRPS. Retrieved from <https://www.chc.ucsb.edu/data/chirps> last accessed on Jan 16, 2024
- Uysal M, Toprak A, Polat N. 2015. DEM generation with UAV Photogrammetry and accuracy analysis in Sahitler hill. *Measurement*, 539-543. <https://doi.org/10.1016/j.measurement.2015.02.018>
- Vericat D, Brasington J, Wheaton J, Cowie M. 2009. Accuracy assessment of aerial photographs acquired using lighter-than-air blimps: low-cost tools for mapping river corridors. *River Research and Applications*, 985-1000. <https://doi.org/10.1002/rra.1243>
- Woodget AS, Carbonneau PE, Visser F, Maddock IP. 2014. Quantifying submerged fluvial topography using hyperspatial resolution UAS imagery and structure from motion photogrammetry. *Earth Surface Processes and Landforms*, 47-64. <https://doi.org/10.1002/esp.3418>
- Young SS, Rao S, Dorey K. 2021. Monitoring The Erosion and Accretion of A Human-built Living Shoreline With Drone Technology. *Environmental Challenges*, 5. <https://doi.org/10.1016/j.envc.2021.100252>